JOURNAL OF MARITIME RESEARCH

Vol XXI. No. III (2024) pp 375–383

ISSN: 1697-4840, www.jmr.unican.es

Experimental Study on Enhancing the Performance of Tidal Energy

Moezeldeen A. Elkeik[1,*], Ahmed Osman[1], Yehia Eldereny[2], Ahmed S. Shehata[2]

ARTICLE INFO

Article history:
Received 27 Aug 2024;
in revised from 05 Sep 2024;
accepted 25 Sep 2024.

Keywords:
Tidal energy, renewable energy, GHG, well turbines.

ABSTRACT

This paper presents the global transition away from fossil fuels and toward renewable energy sources in response to environmental issues, especially climate change. Globally, sustainable energy policies are being put into place to improve reliability of energy, save expenses, and lessen the effects of climate change. A renewable resource that may be found along the coast, tidal energy is becoming more and more popular as a stand-alone option. Tidal barrages are a long-lasting and flexible kind of energy generation since they function according to the rise and fall of the tides. Low head tidal barrage plans do, however, have difficulties in balancing costs and environmental effects. It also discusses the potential and difficulties that come with low head tidal barrage systems, with an emphasis on improving both the viability of the study from an economic and environmental standpoint. Performance evaluation of Wells turbines is part of the study. The blade profile NACA 0015 produced the best performance, according to the data. With a tidal range of one meter, this design reached the greatest spinning speed of 1200 RPM.

1. Introduction.

Since fossil fuel consumption is the primary contributor to climate change and global warming, there is almost no doubt that it has emerged as one of the major issues of the present time (Riahi et al., 2016). The world has recently turned to providing clean sources of energy generation to reduce greenhouse gases emissions (GHG) resulting from burning fossil fuel. Due to their low cost and economic benefits, renewable energy sources are among the greatest and most affordable options for generating power. They are also the ideal substitute for fossil fuels. To moderate global warming and achieve the goals of the Paris Agreement, which are to "avoid dangerous climate change by limiting global warming to well below 2 °C and pursuing efforts to limit it to 1.5 °C," global GHG emissions must rapidly decline (Hickel & Kallis, 2019). The most effective way to reduce GHG emissions is to use renewable energy sources. A crucial renewable source are Earth's oceans, covering 71% of the planet, representing a vast and largely untapped reservoir of renewable energy, harboring over 2000 TW of power (Siagian et al., 2019). Despite the intermittent nature of many renewable technologies, tidal energy emerges as a promising alternative with unique attributes. Unlike other sources, tidal energy stands out for its reliability and predictability, dependent on the gravitational and centrifugal forces among the Earth, moon, and sun. Tidal energy is a sustainable alternative in the mission of reducing CO2 emissions (Hoang et al., 2022). The sun and moon's gravitational pull-on Earth cause the ocean's surface to rise and fall on a regular basis, creating a tide. Due to the moon's smaller distance from Earth than that of the sun, it exerts a gravitational pull that is around 2.2 times stronger than the sun's. The gravitational pull causes two bulges of tides in the earth envelope, one on the side of the earth facing the moon and the other on the opposite side. The location with respect to the earth's rotation axis determines the maximum number of tides that can be witnessed. Tidal ranges are characterized by neap and spring tides. When the earth, moon, and sun are all positioned nearly on the same line during the new and full moon phases, this creates spring tide (Matte et al., 2018). This explains why, during spring tide, tidal ranges are larger than typical. In the meantime,

[1]Marine Engineering Department, College of Engineering and Technology, Arab Academy for Science, Technology and Maritime Transport.

[2]Mechanical Engineering Department, College of Engineering and Technology, Arab Academy for Science, Technology and Maritime Transport.

[*]Corresponding author: Moezeldeen A. Elkeik. E-mail Address: elkeekmoez@gmail.com.

the neap tide happens when the moon is at a 90-degree angle to the sun's gravitational pull. Tidal ranges are smaller than usual during the neap tide. Semi-diurnal tides, diurnal tides, and mixed tides are the three primary forms of the tide phenomena that are influenced by various locations on Earth. The semi-diurnal tides have a duration of 12 hours and 25 minutes, which coincides with the moon's fundamental period (Woodworth et al., 2019). The ocean often experiences two high tides per day during this time. The tide's amplitude changes during the lunar month, with the highest tidal range occurring in semi-diurnal tides. The period of the diurnal tides is equal to one full revolution of the moon around the earth, which lasts for 24 hours and 50 minutes. There is only one high tide of this type per day, which is susceptible to changes brought on by the earth's rotational axis's tilt with respect to the moon's and the earth's orbital planes around the sun. The properties of semi-diurnal and diurnal tides are combined to form the mixed tide, which displays biweekly and monthly variations (Susanto et al., 2018). Figure 1 shows the tidal forms. Tidal energy, harnessed from the natural rise and fall of ocean tides and currents, is considered a highly effective energy source that can meet our annual energy demands (Khojasteh et al., 2017). Despite its underutilization to date, with continued research and development, tidal energy has the potential to become a reliable alternative to traditional energy sources (Bhuiyan, 2022). Tidal energy stands out among renewable energy sources for it predictability and high power density, making it an attractive option in the evolving energy landscape. The predictability and stability of tidal current energy offer advantages over other renewable sources like solar, wind, and biomass energy systems. One effective method of using the tide's potential energy is to build tidal barrages. When a dam is built across a bay or estuary with a tidal range of more than five meters, the potential energy of the tides is captured. This is how tidal barrages work. With the exception of the bidirectional flow of tidal currents, the technique of producing power from tidal barrages is similar to that of hydroelectric generation. Ship locks, embankments, sluice gates, and turbines are the parts of a typical tidal barrage. Turbines used in tidal barrages include bulb turbines, straflo or rim turbines, and tubular turbines. They can be unidirectional or bidirectional. Based on their design and operational framework, tidal barrages are divided into single-basin and double-basin systems. Successful power plants featuring tidal barrages include La Rance (France), Jiangxia (China), Annapolis (Canada), La Rance (France), and Sihwa (South Korea), which is the largest tidal power plant (254 MW). Figure 2 shows the sihwa tidal barrage dam.

Figure 1: Sihwa tidal barrage dam.

Source: Authors.

This study aims to investigate the challenges and opportunities associated with low head tidal barrage schemes and propose solutions for enhancing their economic feasibility and environmental sustainability. This project traces the application of the NACA 0012, 0015, 0018, 0021 designs of Wells turbine in addition to Bulb turbine, Darrius turbine and Savonius turbine, when immersed in a tidal barrage system in order to identify the most efficient type for the generation of tidal energy. Wells turbine is traditionally known for its effectiveness in wave energy converters. Thus, its capabilities are adopted for tidal energy in this project. This study seeks to assess the feasibility and performance of Wells turbines in the context of tidal barrages through experimental model aiming to test multiple designs for the Wells turbine and compare it with other turbine types under the same conditions. The findings will offer new possibilities for renewable energy generation, optimize the right turbine parameters and conditions and provide valuable insights into the potential power generation from this innovative approach to tapping into tidal resources for areas with ultra-low usable head. The results show that the Wells turbine with a NACA0015 blade profile dimension is the most efficient, delivering the highest RPM at 1200 and torque of 1.67 Nm.

2. Methodology

This chapter includes the selected data under experiment as well as the evaluation process and the methodology adopted for this process to occur. Wells turbine performance is evaluated experimentally. The turbine is going to be installed in a tube between two tanks with a head difference, which resembles the tide. First, the wells turbine will be 3D-modelled and scaled by a factor of 0.233 using SolidWorks using a high solidity wells turbine prototype as a reference (Mishra et al., 2018) along with a Bulb turbine, Darrieus turbine used by Rodolfo in his experiment scaled by a factor of 0.571 and Savonius turbine used by Golecha Kailash in his experiment scaled by a factor of 0.408 for comparison. Multiple wells turbine designs with different blade profiles will be simulated to determine the optimum design for the turbine. The turbine's performance under different heads will be monitored through its rotational speed and torque,

the power generated and efficiency will be calculated and compared with the other turbine tested to prove its significance.To calculate the potential energy available in the tide, the gross energy potential E_f (J) for a single tidal basin is calculated using the following equations

$$E_f = \rho\, g \int_{Z=0}^{Z=R} Z\, A_z\ dZ \tag{1}$$

$$E_f = \rho\, g\, A_z \int_{Z=0}^{Z=R} Z\ dZ \tag{2}$$

$$E_f = \rho\, g\, A_z\, \frac{R^2}{2} \tag{3}$$

Where A_z is the basin area (km^2), ρ is the sea water density (kg/m^3), g is the gravitational acceleration (9.81 m/s^2), and R is the tidal range difference (m).

The potential energy in the seawater basin at high tide is:

$$E_f = (1024\ \mathrm{kg}/m^3) \times (9.81\ \mathrm{m}/s^2) \times (1 \times 10^6\ m^2)\ \times \frac{(1.1\ m)^2}{2} \tag{4}$$

$$E_f = 6.07774912\ \times 10^9\ J \tag{5}$$

Since there are two tidal cycles per day, two high and two low tides, the total potential energy in a single day is:

$$E_T = \left(6.0774912\ \times 10^9\ J\right) \times 2 = 1.21549824\ \times 10^{10}\ J \tag{6}$$

At low tide Potential Energy is equal zero. Thus, the mean power available per day in tidal range is:

$$P_T = \frac{(1.21549824\ \times 10^{10}\ J)}{(86400\ s/day)} = 140.683\ kW \tag{7}$$

Assuming turbine efficiency to be 80%, the electrical power generated will be:

$$P_T = (140.683\ kW) \times 0.8 = 112.546\ kW \tag{8}$$

The electrical power calculated is for one turbine per square kilometer tidal basin area.

The primary objective of the experiment is to determine the most suitable turbine for ultra-low heads application. This involves testing various turbines, including Wells turbines with multiple blade profiles including NACA0012, NACA0015, NACA0018, NACA0021, as well as Bulb turbine, Darrieus turbine and Savonius turbine. Figure 2 shows the Experimental Setup Design and figure 3 shows the Turbine Tunnel Design.

Figure 2: Experimental Setup Design.

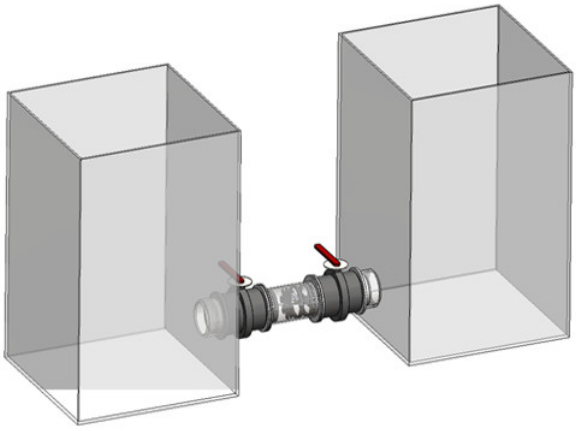

Source: Authors.

Figure 3: Turbine Tunnel Design.

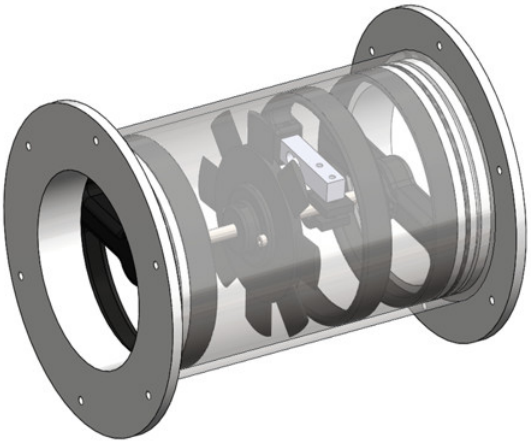

Source: Authors.

Figure 4 shows the Actual Setup Design under experiment.

Figure 4: Actual Setup Design under experiment.

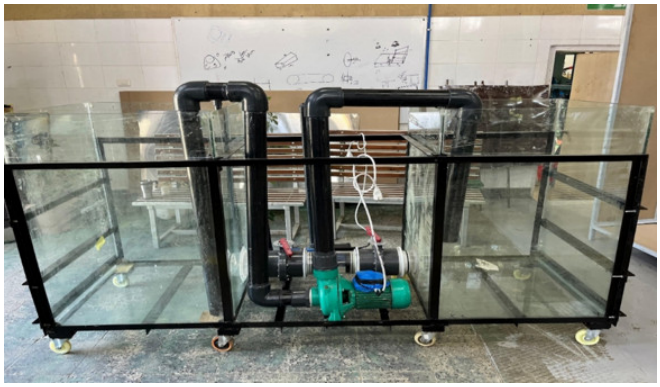

Source: Authors.

Table 1 shows the list of equipment used in the experiment.

Table 1: List of equipment used in the experiment.

Component	*Material*	*Dimensions*	*Number of items*	*Notes*
Tank	Glass	L=80cm,w=80cm,H=120	2	
Turbine tunnel	Acrylic	L=30cm,ID=6 inch	1	
Turbines	PLA	OD=13.8 cm	1	
Supports	PLA	14 cm	2	
Bearing	Stainless Steel	ID=8mm , OD=22mm	6	
Flange	Artelon	OD = 20 cm, ID = 14 cm	6	
Gaskets	Rubber	OD = 20 cm, ID = 14 cm	2	
Pipes	PVC	3 inch × 5m	1	
Bolts	Steel	M5	12	
Nuts	Steel	M5	12	
Wahers	Steel	M5	12	
O-ring	Rubber	6 inch	8	
Butterfly valve	PVC	6 inch	2	
Rod	Stainless Steel	D=8mm, L=19cm & 12 cm	1	
Pump	Cast Iron	2 HP	1	
Arduino System	-	-	1	

Source: Authors.

For the system calculations, H_1 and H_2 are the heads in meters in Tanks 1 and 2 respectively the difference between H2 and H1 is one meter.

$$h_{losses} = h_{major} + h_{minor} \tag{9}$$

$$h_{major} = f * (\frac{L*v^2}{D*2g}) \tag{10}$$

$$h_{minor} = k_c *(\frac{v^2}{2g})+k_E *(\frac{v^2}{2g})+4k_{elbow}*(\frac{v^2}{2g})+2k_v *(\frac{v^2}{2g}) \tag{11}$$

Where h_{major} is the losses due to pipe friction, h_{minor} is the losses due to piping accessories, h_{Losses} is the total system losses in meters, f is the friction factor = 0.0015 (assumption), L is the length of the Pipes in the system = 2 meters, D is the diameter of the Pipes = 6 inch (0.1524 m), k_c is the losses coefficient for contraction between tank 1 and pipe = 0.5 (max), k_E is the losses coefficient for enlargement between pipe and tank 2 = 1 (max), and k_v is the losses coefficient for a butterfly valve = 0.73.

$$Q = A \times v = \frac{\pi}{4} \times D^2 \times v \tag{12}$$

Q is the flow rate of the system (m^3/s), A is the area of the turbine tunnel (m^2), and D is the diameter of the turbine tunnel (0.1524 m). Velocity in turbine tunnel (v) is *2.566 m/s* and Flow rate of system (*Q) is 0.0468 m^3/s.*

The Hydraulic Power in the water is:

$$P_H = \rho g h Q \tag{13}$$

ρ is the water density in the system (1000 kg/m^3), g is the gravitational acceleration (9.81 m/s^2), and h is the head difference (1 m). Hydraulic Power *is 459.191 Watt*, Assuming turbine efficiency (ηT) to be 80%. The Electrical Power generated (PE) will be 367.353 Watt.

3. Experimental Procedures.

The Wells Turbine is Compact Energy Extraction that efficiently harnesses power from reciprocating air flows. Its design, featuring symmetric aerofoil blades set at 90-degree angles around a central hub, ensures optimal energy capture. This axial-flow turbine's aerodynamics enables it to be self-rectifying. This unique feature enables unidirectional rotation without additional rectification systems. Its high specific speed, with uncambered aerofoils on a rotor, optimizes energy extraction. This expirement is made to give reads for the tidal range all over the Egyption coast. It is important to decide which turbine is going to be used after changing the heads several times and comparing the results to decide which turbine will give the best effiency and then be used. The tested turbines are Wells turbine, Bulb turbine, Darrieus turbine, and Savonius turbine.

Begin by setting up the experimental apparatus, including tanks 1 and 2, the intermediate pipe, turbine, valve, and Torque meter and tachometer.

Ensure that the turbine to be tested is properly installed in the system.

3.1. Trial 1: Filling Tank 1 with Head Difference.

1. Fill tank 1 and 2 with water, utilizing the specific head difference required for the trial in Tank A.
2. Close the valve for tank 2 to prevent water flow from tank 1 to tank 2 during the filling process.
3. Once the required head is achieved in tank 1, open the valve to allow water to flow through the intermediate pipe and rotate the turbine; at the same time turn on the pump to make the experiment operate for a longer time.
4. Use the tachometer to determine the speed and record them in a table.
5. After a few minutes, when both tanks have the same water level, the trial is complete.

3.2. Trial 2: Filling Tank 2 with Head Difference.

1. Transfer water from tank 1 to tank 2 by using a pump installed in the system while using the valve to prevent backflow.
2. Repeat steps 4-7 for head difference in tank 2.

3.3. Testing a New Turbine.

1. Close the valves to prevent water flow.
2. Empty the intermediate pipe by removing any remaining water.
3. Remove the turbine used in the previous trial to prepare for the next turbine test.
4. Install the new turbine to be tested in the system.
5. Repeat steps 3-7 for the new turbine, following the same procedure as in Trial 1.

4. Results and discussion

This study aimed to evaluate the performance of four different turbine types including: Bulb turbine, Darrieus turbine, Savonius turbine and Wells turbine in low head tidal barrage applications. Through a series of controlled experiments, we measured and compared the rotational speed (RPM) at multiple head differences for each turbine. The findings highlight significant differences in these parameters, providing insights into the efficiency and suitability of each turbine for low head tidal energy systems. The findings for each turbine are shown below:

Table 2: Bulb turbine RPM at various head differences.

Head Difference (cm)	*RPM*
0	0
7	120
12	420
23	480
26	480
46	660
62	680
81	720
100	900

Source: Authors.

Figure 5: Bulb turbine graph.

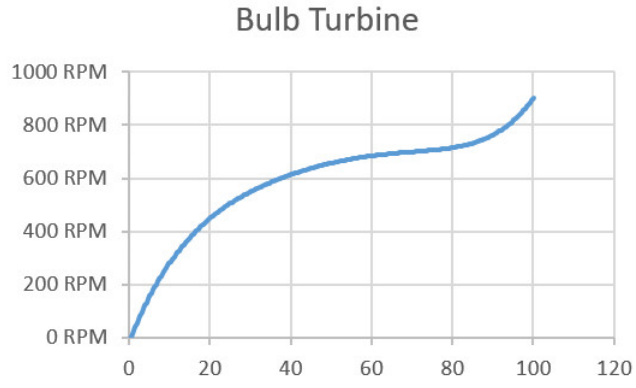

Source: Authors.

Table 3: Darrieus turbine RPM at various head differences.

Head Difference (cm)	*RPM*
0	0
2	60
6	60
15	240
17	240
20	240
23	300
25	300
29	360
34	360
37	420
43	420
47	420
53	450
61	450
79	480
100	600

Source: Authors.

Figure 6: Darrieus turbine graph.

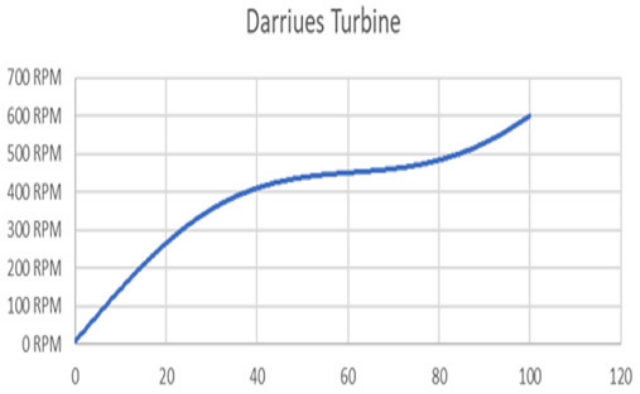

Source: Authors.

Table 4: Savonius turbine RPM at various head differences.

Head Difference (cm)	*RPM*
0	0
7	120
12	240
16	300
20	300
38	480
75	600
100	840

Source: Authors.

Figure 7: Savonius turbine graph.

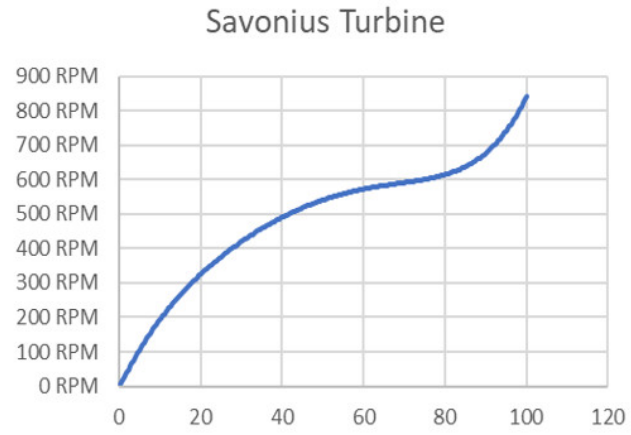

Source: Authors.

Table 5: Wells turbine (NACA0015) readings at various head differences.

Head Difference (cm)	*RPM*	*Torque (Nm)*	*Flow rate(m³/sec)*	*Efficiency (%)*
0	*0*	*0*	*0*	*0*
9	*120*	*0.44*	*0.02045*	*30.61*
18	*240*	*0.88*	*0.02892*	*43.29*
39	*280*	*1.45*	*0.04258*	*26.09*
80	*1020*	*1.5*	*0.06098*	*33.47*
100	*1200*	*1.67*	*0.06818*	*31.37*

Source: Authors.

Figure 8: Wells turbine (NACA0015) RPM graph.

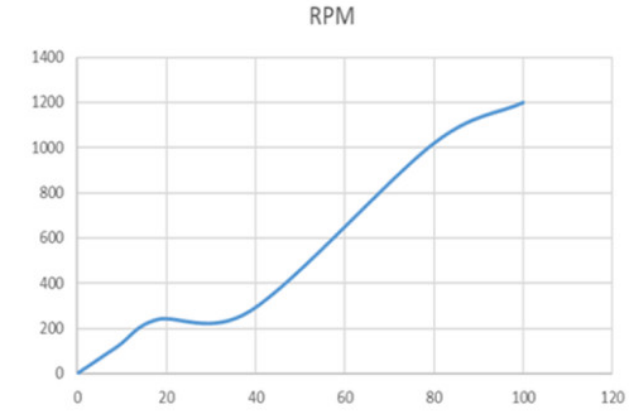

Source: Authors.

The findings of the experiment revealed that the Wells turbine achieved the highest RPM compared to the bulb, Darrius, and Savonius turbines, indicating its superior performance in low head tidal barrage applications. Given these promising results, the Wells turbine was further examined by altering the blade profile using NACA0012, NACA0015, NACA0018, and NACA0021 airfoil shapes. This modification aimed to identify the optimum blade profile that maximizes efficiency and performance.

Figure 9: Wells turbine (NACA0015) Torque graph.

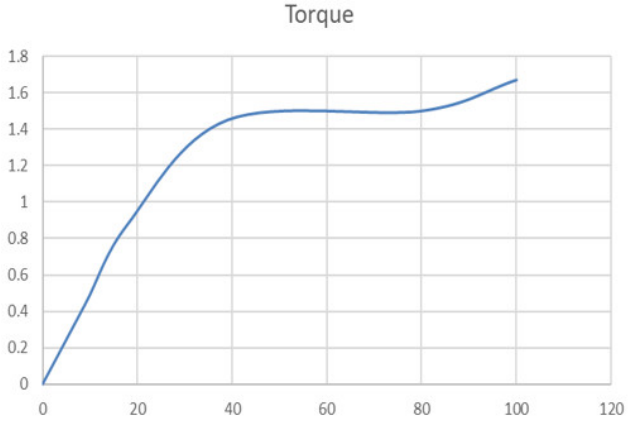

Source: Authors.

Figure 10: Wells turbine (NACA0015) efficiency graph.

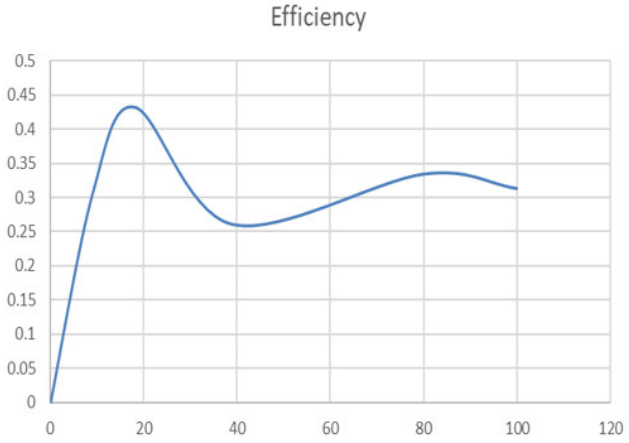

Source: Authors.

Table 6: Wells turbine (NACA0012) readings at various head differences.

Head Difference (cm)	*RPM*	*Torque (Nm)*	*Flow rate (m³/sec)*	*Efficiency (%)*
0	0	0	0	0
8	110	0.21	0.01928	15.98
13	120	0.29	0.02458	11.62
21	230	0.67	0.03124	25.06
29	440	0.89	0.03671	39.25
47	510	1.1	0.04674	27.25
58	535	1.15	0.05192	21.81
74	890	1.4	0.05865	30.64
100	1071	1.57	0.06818	26.32

Source: Authors.

For this purpose, we measured the RPM and torque at various head differences, which enabled us to calculate the flow rate and turbine efficiency. By systematically varying the blade profiles, we sought to understand their impact on the turbine's hydrodynamic characteristics and overall energy extraction capability. The results of these tests provide a detailed analysis of how each blade profile influences the Wells turbine's performance, helping to identify the most effective design for maximizing tidal energy yield in low head conditions. The detailed findings, including RPM, torque, flow rate, and efficiency data, are presented below:

Figure 11: Wells turbine (NACA0012) RPM graph.

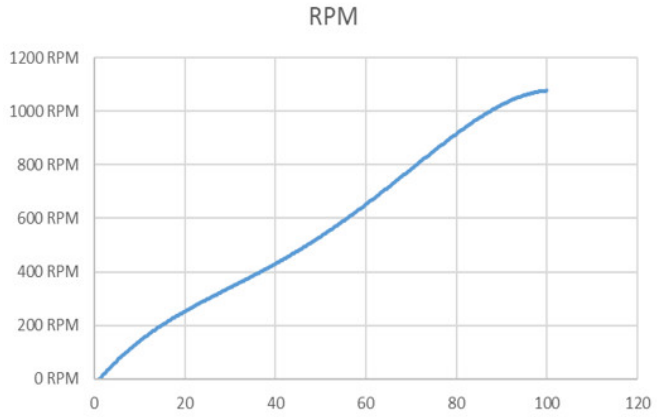

Source: Authors.

Figure 12: Wells turbine (NACA0012) Torque graph.

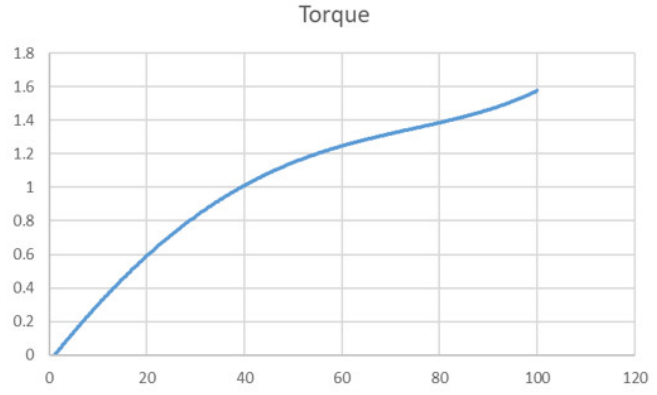

Source: Authors.

After conducting numerous experiments on various configurations of the Wells turbine, we extensively modified the blade profile sizes to observe their impact on performance. We adjusted the blade dimensions to NACA 0015, NACA 0012, NACA 0018, and NACA 0021 of the turbine's cord length of the maximum diameter. Following thorough examination and testing of these different configurations, we arrived at several significant findings. Results indicate that the blade profile NACA 0015 yielded the most favorable outcomes. This configuration achieved the highest rotational speed, reaching 1200 RPM at a tidal range of 1 meter. In comparison, other turbine configurations produced similar results but consistently fell short of the NACA0015 blade profile's performance.

Figure 13: Wells turbine (NACA0012) Efficiency graph.

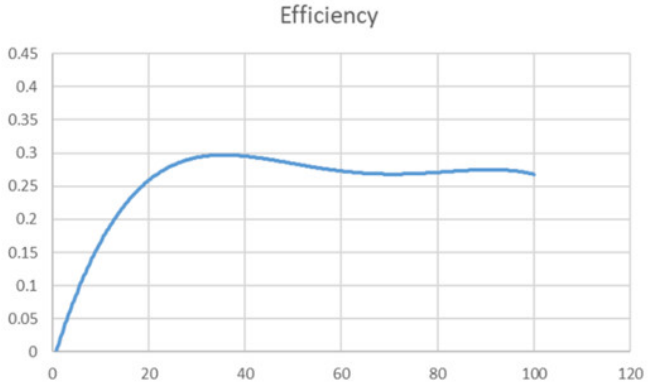

Source: Authors.

Table 7: Wells turbine (NACA0018) readings at various head differences.

Head Difference (cm)	*RPM*	*Torque (Nm)*	*Flow rate (m^3/sec)*	*Efficiency (%)*
0	0	0	0	0
5	60	0.3	0.01524	25.21
11	240	0.42	0.02261	43.25
20	300	0.56	0.03049	29.41
38	480	0.71	0.04203	22.77
62	540	0.82	0.05368	14.19
79	540	0.82	0.06060	9.87
100	780	1.01	0.06818	12.33

Source: Authors.

Figure 14: Wells turbine (NACA0018) RPM graph.

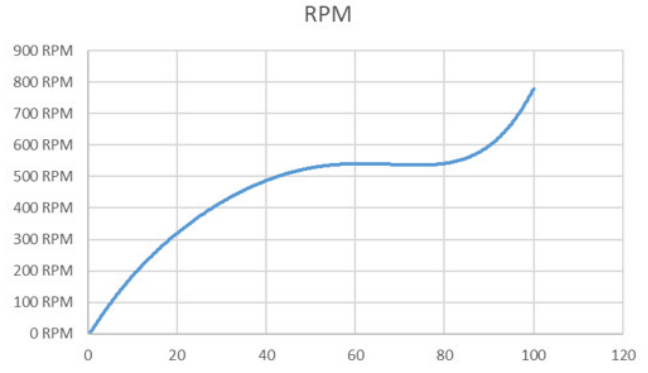

Source: Authors.

Figure 15: Wells turbine (NACA0018) Torque graph.

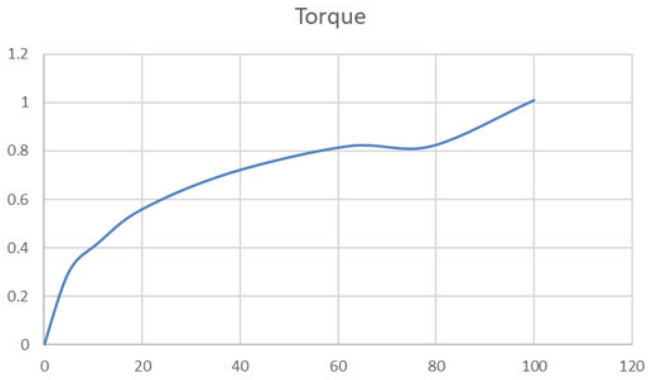

Source: Authors.

Figure 16: Wells turbine (NACA0018) Efficiency graph.

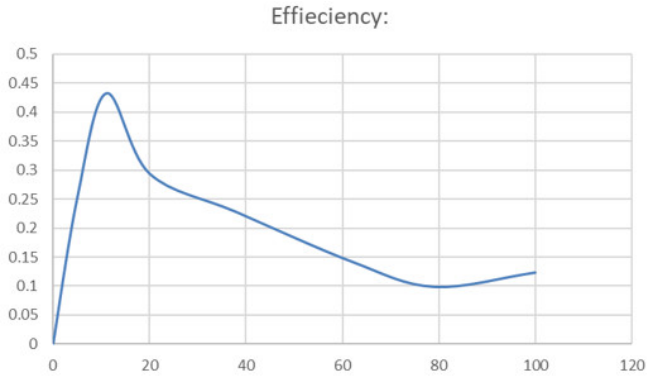

Source: Authors.

Table 8: Wells turbine (NACA0021) readings at various head differences.

Head Difference (cm)	*RPM*	*Torque (Nm)*	*Flow rate (m^3/sec)*	*Efficiency (%)*
0	0	0	0	0
10	180	0.25	0.02156	22.27
20	300	0.5	0.03049	26.25
22	360	0.53	0.03198	28.94
32	420	0.71	0.03857	25.78
55	540	1.01	0.05056	20.93
66	660	1.2	0.05539	23.12
70	900	1.26	0.05704	30.31
100	960	1.4	0.06818	21.04

Source: Authors.

Figure 17: Wells turbine (NACA0021) RPM graph.

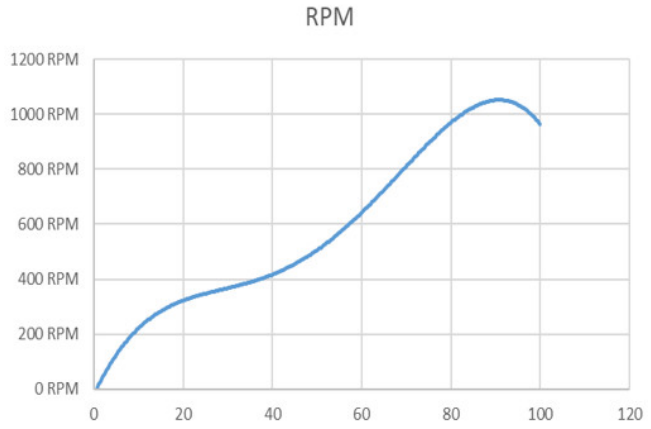

Source: Authors.

Figure 18: Wells turbine (NACA0021) Torque graph.

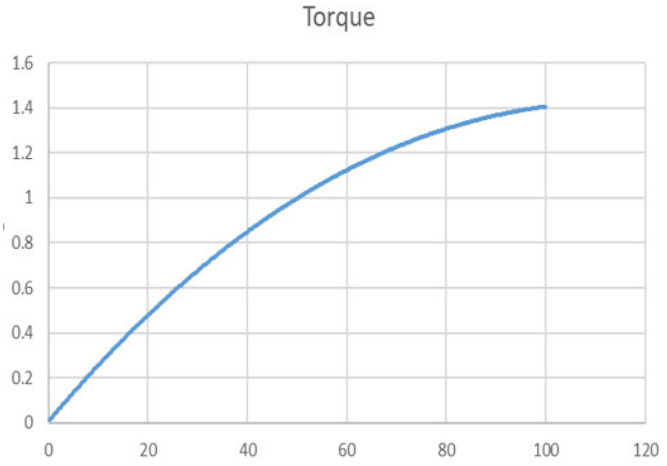

Source: Authors.

Figure 19: Wells turbine (NACA0021) Efficiency graph.

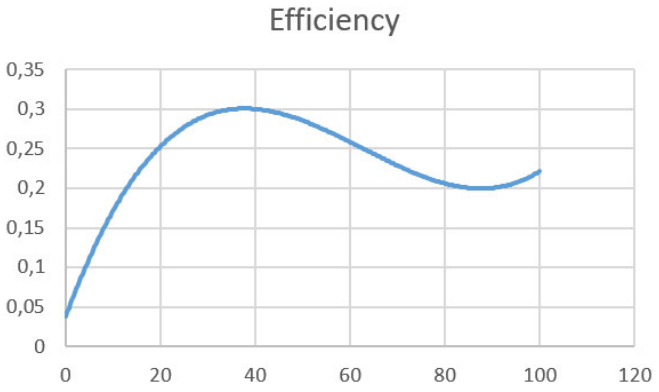

Source: Authors.

Conclusions.

The study introduces the global shift towards renewable energy solutions in response to the depletion of fossil fuels and environmental concerns, particularly climate change. Sustainable energy policies are being implemented worldwide to enhance energy security, reduce costs, and mitigate the impact of climate change. Tidal energy, a renewable source found along the shore, is emerging as a promising alternative with unique attributes. Tidal barrages operate based on the rise and fall of tides, showcasing longevity and adaptability in energy production. However, low head tidal barrage schemes face challenges related to balancing costs and environmental impacts. It also addresses the challenges and opportunities associated with low head tidal barrage schemes, focusing on enhancing economic feasibility and environmental sustainability. The study aims to assess the feasibility and performance of Wells turbines in the context of tidal barrages through experimental, comparing multiple turbine designs to optimize renewable energy generation from tidal resources. It also discusses the economic feasibility limitations, environmental impacts and hydrodynamic challenges associated with low head tidal barrage schemes.

Research on various turbine types for tidal energy generation has been conducted, but there is a notable gap in comprehensive studies focusing on the application of Wells, Bulb, Darrius, and Savonius turbines within low head tidal barrage systems to maximize energy production economically and sustainably. This area presents a significant opportunity for investigation to evaluate the performance of these turbine designs and propose innovative solutions for enhancing their viability as renewable energy sources. The study involves evaluating Wells turbine performance. results indicate that the blade profile NACA 0015 yielded the most favorable outcomes. This configuration achieved the highest rotational speed, reaching 1200 RPM at a tidal range of 1 meter. In comparison, other turbine configurations produced similar results but consistently fell short of the NACA0015 blade profile's performance.

References.

1. Siagian, H., Sugianto, D. N., & Kunarso, N. (2019). Current Velocity Impacts from Interaction of Semidiurnal and Diurnal Tidal Constituents for Tidal Stream Energy in East Flores. IOP Conference Series Earth and Environmental Science, 246, 012056. https://doi.org/10.1088/1755-1315/246/1/012056.
2. Hoang, A. T., Foley, A. M., Nižetić, S., Huang, Z., Ong, H. C., Ölçer, A. I., Pham, V. V., & Nguyen, X. P. (2022). Energy-related approach for reduction of CO2 emissions: A critical strategy on the port-to-ship pathway. Journal of Cleaner Production, 355, 131772. https://doi.org/10.1016/j.jclepro.2022.131772.
3. Susanto, R. D., Pan, J., & Devlin, A. T. (2018). Tidal Mixing Signatures in the Hong Kong Coastal Waters from Satellite-Derived Sea Surface Temperature. Remote Sensing, 11(1), 5. https://doi.org/10.3390/rs11010005
4. Khojasteh, D., Khojasteh, D., Kamali, R., Beyene, A., & Iglesias, G. (2017). Assessment of renewable energy resources in Iran; with a focus on wave and tidal energy. Renewable and Sustainable Energy Reviews, 81, 2992–3005. https://doi.org/10.1016/j.rser.2017.06.110.
5. Mishra, N., Gupta, A. S., Dawar, J., Kumar, A., & Mitra, S. (2018). Numerical and experimental study on performance enhancement of Darrieus vertical axis wind turbine with WingTip devices. Journal of Energy Resources Technology, 140(12). https://doi.org/10.1115/1.4040506
6. Riahi, K., Van Vuuren, D. P., Kriegler, E., Edmonds, J., O'Neill, B. C., Fujimori, S., Bauer, N., Calvin, K., Dellink, R., Fricko, O., Lutz, W., Popp, A., Cuaresma, J. C., Kc, S., Leimbach, M., Jiang, L., Kram, T., Rao, S., Emmerling, J., Tavoni, M. (2016). The Shared Socioeconomic Pathways and their energy, land use, and greenhouse gas emissions implications: An overview. Global Environmental Change, 42, 153–168. https://doi.org/10.1016/j.gloenvcha.2016.05.009.
7. Hickel, J., & Kallis, G. (2019). Is green growth possible? New Political Economy, 25(4), 469–486. https://doi.org/10.1080/13563467.2019.1598964.
8. Matte, P., Secretan, Y., & Morin, J. (2018). Drivers of residual and tidal flow variability in the St. Lawrence fluvial estuary: Influence on tidal wave propagation. Continental Shelf Research, 174, 158–173. https://doi.org/10.1016/j.csr.2018.12.008.
9. Woodworth, P. L., Melet, A., Marcos, M., Ray, R. D., Wöppelmann, G., Sasaki, Y. N., Cirano, M., Hibbert, A., Huthnance, J. M., Monserrat, S., & Merrifield, M. A. (2019). Forcing factors affecting sea level changes at the coast. Surveys in Geophysics, 40(6), 1351–1397. https://doi.org/10.1007/s10712-019-09531-1.
10. Bhuiyan, M. R. A. (2022). Overcome the future environmental challenges through sustainable and renewable energy resources. Micro & Nano Letters, 17(14), 402–416. https://doi.org/10.1049/mna2.12148.